Effect of design and growth conditions of metamorphic In(Ga,Al)As/GaAs heterostructures on electrical properties of $In_{0.75}Ga_{0.25}As$/InAlAs two-dimensional channel

© M.Yu. Chernov, V.A. Solov'ev, I.L. Drichko, I.Yu. Smirnov, S.V. Ivanov

Ioffe Institute,
191021 St. Petersburg, Russia

E-mail: chernov@beam.ioffe.ru

Received May 7, 2024
Revised May 12, 2024
Accepted May 13, 2024

Undoped metamorphic structures with $In_{0.75}Ga_{0.25}As$ quantum well and various design of (In,Al)As barriers were grown on GaAs substrates by molecular beam epitaxy. Electrical properties of such structures were studied by using a 4-point Van der Pauw method and contactless technique based on the analysis of propagation of surface acoustic waves along the interface of the piezoelectric $LiNbO_3$ and the sample. Increasing the thickness of the bottom barrier layer of the $In_{0.75}Ga_{0.25}As$ quantum well as well as optimizing the growth temperature and As_4/III ratio allowed achieving concentration and mobility of 2D carriers in 30 nm−thick $In_{0.75}Ga_{0.25}As$ QW of below $3.4 \cdot 10^{11}$ cm^{-2} and above $2 \cdot 10^5$ cm^2/(V · s), respectively, at $T = 1.7$ K.

Keywords: molecular beam epitaxy, metamorphic heterostructures, metamorphic buffer layer, two-dimensional electron channel, InGaAs/InAlAs.

DOI: 10.61011/SC.2024.03.58838.6653

1. Introduction

InGaAs/InAlAs heterostructures are widely used in VHF electronics [1,2]. In particular, HEMT transistors based on $In_{0.7}Ga_{0.3}As/In_{0.52}Al_{0.48}As$ heterostructures, created on InP substrates, have record-breaking performance and minimal noise characteristics to date [3,4]. Obtaining structures with $In_xGa_{1-x}As$ ($x > 0.7$) quantum wells (QW) on GaAs substrates has been of a particular interest recently as they differ from InP by higher manufacturability and lower cost. At the same time, the high dislocation density arising in the structures, because of the strong mismatch of the parameters of the crystal lattice of the GaAs substrate and the two-dimensional channel of $In_xGa_{1-x}As$ ($x > 0.7$) ($\Delta a/a > 5\%$), has a negative impact on the output characteristics of devices based on them. Metamorphic growth technology is used for solving this problem which is based on the use of a metamorphic buffer layer (MBL) of a solid solution of variable composition for creation of a low-defect, elastic stress-free virtual substrate (VS) [5]. VS is necessary for the formation of pseudomorphic layers on it, including a two-dimensional electronic channel. The electrophysical parameters of a 2D channel, such as the concentration and mobility of carriers, strongly depend on its design and technological conditions of growth. For instance, it has been shown that it is possible to control the concentration of carriers in 30 nm thick undoped QW of $In_{0.75}Ga_{0.25}As/In_{0.75}Al_{0.25}As$ from $2 \cdot 10^{11}$ cm^{-2} to more than $4 \cdot 10^{11}$ cm^{-2} by changing the conditions of molecular beam epitaxy (MBE) of growth [6]. In this case, an important task is to ensure a high carrier mobility in the channel at a concentration corresponding to occupation of only the first level of dimensional quantization for avoiding the intersubband scattering of carriers.

This paper is devoted to the study of the electrophysical characteristics of metamorphic structures of the original design with a two-dimensional electronic channel of $In_{0.75}Ga_{0.25}As$ obtained by the MBE method on GaAs substrates, depending on the design of barrier layers (In,Al)As and MBE growth conditions (growth temperature and ratio of streams As_4/III).

2. Experiment

A series of metamorphic heterostructures of In(Ga,Al)As (samples A−E) was obtained using the MBE method on undoped GaAs(001) substrates using the RIBER 32P system, the schematic design of which is shown in Figure 1. Samples A, B and C contained successively from a substrate a GaAs buffer layer (200 nm), $In_xAl_{1-x}As$ metamorphic buffer layer (MBL), the composition of which varied according to the root law (1 μm), the virtual substrate being the lower barrier layer, which comprised a superlattice (SL) of 1 nm−InAs/4 nm−$In_{0.7}Al_{0.3}As$, $In_{0.75}Ga_{0.25}As$ QW (30 nm), upper barrier layer — SL of 1 nm−InAs/4 nm−$In_{0.7}Al_{0.3}As$ (105 nm) and the covering layer of $In_{0.75}Ga_{0.25}As$ (5 nm). The design of the samples D and E differed from samples A, B and C in the type of barrier layers used. For instance, the function of barrier layers in samples D and E was performed by a triple solid solution of $In_{0.75}Al_{0.25}As$. $In_xAl_{1-x}As$ MBL, the composition of which changed according to the root law of $x = x_{\min} + (x_{\max} - x_{\min})(l/l_t)^{1/2}$, where $x_{\min} = 0.05$ and $x_{\max}$ — initial and final contents of In in the MBL, respectively, and l_t — its thickness was used in all structures studied in this work, since its effectiveness in reducing the

Table 1. Distinctive features of the design and conditions of MBE growth of the studied metamorphic heterostructures (samples A–E)

Sample	Lower barrier layer of QW of $In_{0.75}Ga_{0.25}As$ (virtual substrate)	Thickness of the lower barrier layer, nm	MBE growth conditions of 2D channel	
			T_s, °C	As_4/III
A	CP 1 nm–InAs/4 nm–$In_{0.7}Al_{0.3}As$	40	480	13
B	CP 1 nm–InAs/4 nm–$In_{0.7}Al_{0.3}As$	60	480	13
C	CP 1 nm–InAs/4 nm–$In_{0.7}Al_{0.3}As$	60	480	10
D	$In_{0.75}Al_{0.25}As$	120	450	10
E	$In_{0.75}Al_{0.25}As$	120	450	8

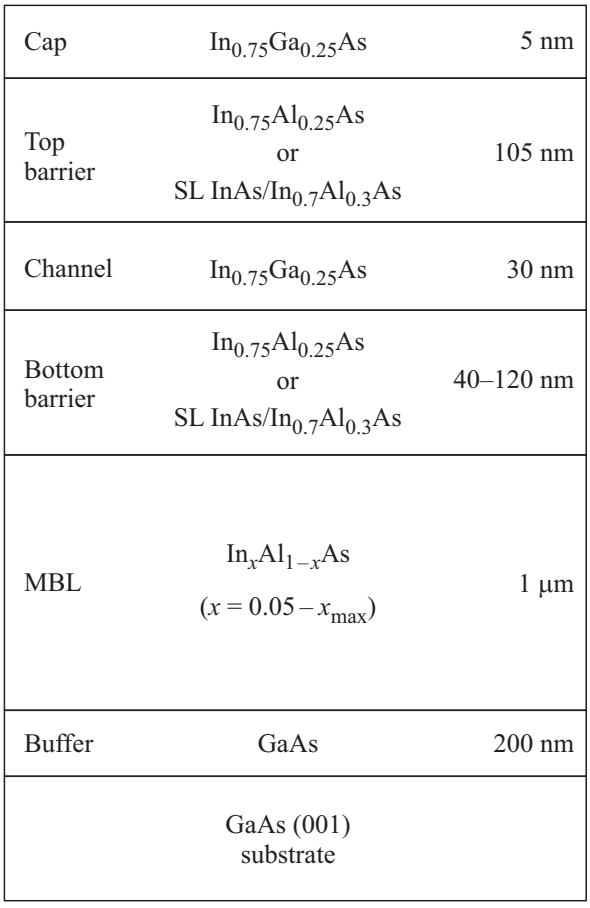

Figure 1. Schematic design of the studied metamorphic heterostructures In(Ga,Al)As/GaAs with a two-dimensional channel of $In_{0.75}Ga_{0.25}As$.

density of threading dislocations was previously demonstrated compared to MBL with a stepped or linear profile of the composition change [7]. The value of the inverse step, representing the difference between the final composition of the MBL and the composition of the virtual substrate (VS), was chosen to be $\Delta x = 0.05$ for samples A, B, C and 0.06 for samples D and E. It was previously shown that the inverse step $\Delta x = 0.05–0.06$ in case of usage of MBL with a root profile of composition change makes it possible to realize an elastically stressed VS and avoid relaxation of elastic mechanical stresses in layers grown over the VS [8]. Therefore, the final In content in InAlAs MBL was $x_{max} = 0.75$ in samples A–C and 0.81 in samples D and E. The thickness of the VS varied in the range of 40–120 nm (see Table 1). It was assumed that using SL of InAs/4 nm–$In_{0.7}Al_{0.3}As$ as an VS would reduce the density of threading dislocations in a two-dimensional channel and thereby improve its electrophysical characteristics.

The growth of all structures studied in this work began with the procedure of low-temperature ($T_s < 500$°C) annealing of GaAs substrates in a Ga stream. It was demonstrated that the reaction of conversion of oxide Ga_2O_3 into Ga_2O effectively takes place during such annealing, and the surface becomes significantly more planar than in case of a standard high-temperature annealing when the Ga atoms necessary for this reactions are taken from the substrate, creating pits in it [9]. The MBE conditions for the growth of InAlAs MBL were similar to those given in Ref. [10]. The temperature of growth of the two-dimensional channel of $In_{0.75}Ga_{0.25}As$ and barrier layers (In,Al)As varied in the range of $T_s = 450–480$°C and was controlled by an IR pyrometer (IRCON). The pyrometer was calibrated prior to the MBL growth based on the change of the reconstruction of the GaAs surface $((2 \times 4)As \rightarrow c(4 \times 4)As)$ using the diffraction of fast reflected electrons. This reconstruction is well known and occurs at $T_s = 500–520$°C depending on the pressure of the incident stream of As_4 [11]. The ratio of streams of element of groups V and III during the growth of $In_{0.75}Ga_{0.25}As$ and barrier layers (In,Al)As varied in the range of $As_4/III = 8 - 13$. The growth rate of all layers in the structures was 0.7 ML/s. ML means a monolayer. The distinctive features of the design and conditions of the MBE growth of samples A–E are given in Table 1.

Two methods were used to determine the electrophysical parameters of the 2D channel of $In_{0.75}Ga_{0.25}As$, such as electron concentration and mobility: 1) four-contact van der Pauw method for measurements at $T = 80$ and 300 K (for all samples) and 2) a non-contact method based on the analysis of the propagation of surface acoustic waves (SAW) along the interface of the piezoelectric $LiNbO_3$ and the sample [12], for measurements at $T = 1.7$ K (for samples A, C and E).

The scheme of the acoustic experimental setup is shown in Figure 2. The sample is pressed by a spring against the surface of a lithium niobate plate ($LiNbO_3$), on both sides of which interdigital transducers are formed for the generation and detection of SAW. Then, the SAW is excited by applying an alternating voltage U_{in} to the IDT1 interdigital transducer due to the piezoelectric effect on the $LiNbO_3$ surface. The wave is accompanied by an alternating electric field, which penetrates into a two-dimensional channel and causes currents of charge carriers, which in turn cause Joule losses.

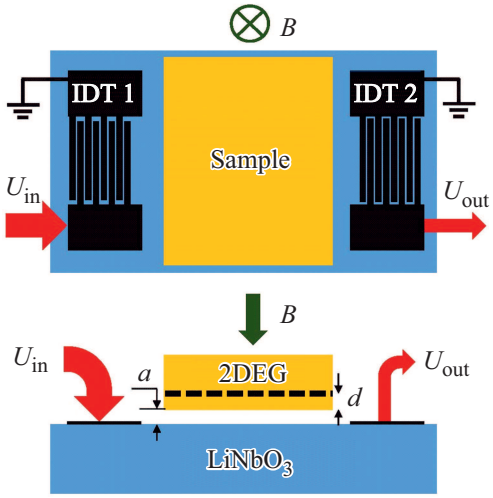

Figure 2. Scheme of the acoustic experimental setup: top view (top panel) and side view (bottom panel).

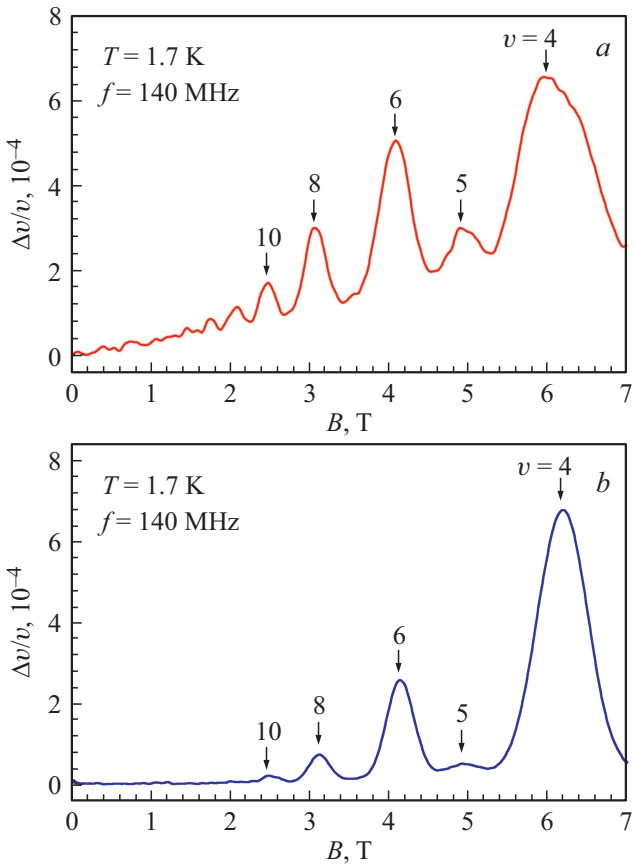

Figure 3. Dependencies of absorption Γ (a) and changes of velocity $\Delta v/v$ (b) of SAW on the magnetic field obtained for the sample A with the SAW frequency of $f = 140$ MHz. $\nu = 2E_F/\hbar\omega_c$ — occupation number, where E_F — Fermi energy, $\omega_c = eB/m^*c$ — cyclotron frequency.

The interaction of the electric field of the SAW with electrons in the 2D channel results in a change of the amplitude and phase shift of the SAW, which are recorded by the second IDT2 interdigital transducer. In this case, the deformation is not transmitted to the sample from the SAW. The acoustic setup was placed in a helium cryostat with a superconducting magnet. The absorption (Γ) and changes of velocity ($\Delta v/v$) of SAW were measured at a SAW frequency equal to 140 MHz in a transverse magnetic field of $B \leq 8$ T. An example of the dependencies of $\Gamma(B)$ and $\Delta v/v(B)$ obtained for sample A at $T = 1.7$ K, is shown in Figure 3. The arrows on Figure 3 indicate the occupation numbers. Similar dependences were obtained for samples C and E.

3. Results and discussion

Figure 4 shows the dependences of the real (σ_1) and imaginary (σ_2) parts of the high-frequency conductivity ($\sigma^{AC} = \sigma_1 - i\sigma_2$) on the magnetic field for samples A (a), C (b) and E (c) at $T = 1.7$ K, calculated from the obtained experimental dependencies $\Gamma(B)$ and $\Delta v/v(B)$ in accordance with Ref. [13]. It was previously found that the case of $\sigma_1 < \sigma_2$ corresponds to a hopping type of conductivity when carriers are localized at a random impurity/defect potential, while the case of $\sigma_1 > \sigma_2$ indicates conductivity attributable to delocalized carriers [14]. It should be noted that on all dependencies $\sigma_{1,2}(B)$ obtained for samples A, C and E at $T = 1.7$ K (Figure 4), the real part of the conductivity (σ_1) prevails over the imaginary (σ_2) with $B \leq 3$ T (area of fields where Shubnikov-de Haas oscillations are observed), which allows making a conclusion that there are no effects of carrier localization in a two-dimensional channel and indirectly indicates the high crystal perfection of the studied structures. The quantum Hall effect mode is implemented in the studied samples with $B > 3$ T. The concentration of electrons (n) in the 2D channel of samples A, C and E at $T = 1.7$ K was determined from the position of the minima of the Shubnikov-de Haas oscillations in the magnetic field (Figure 4) (see Table 2). The non-oscillating part of the actual conductivity component was calculated to determine the electron mobility (Figure 5) in accordance with the expressions (1) given in Ref. [15]:

$$\sigma_1(B) = \sigma_1^1(B) + \sigma_1^{osc}(B),$$

$$\sigma_1^1(B) = \frac{en\mu c^2}{\mu^2 B^2} \quad (\omega_c\tau = \mu B/c \gg 1), \qquad (1)$$

where σ_1^1 and σ_1^{osc} — the oscillating and non-oscillating parts of the actual component of high-frequency conducti-

Table 2. Concentration and mobility of electrons in 2D channel of $In_{0.75}Ga_{0.25}As$ of metamorphic heterostructures at $T = 1.7$, 80 and 300 K and 2D channel growth parameters

Sample	T, K						MBE conditions of growth of 2D channel	
	n, 10^{11} cm^{-2}			μ, cm^2/(B · c)				
	300	80	1.7	300	80	1.7	T_s, °C	As_4/III
A	8.1	6.7	5.9	11200	73300	210000	480	13
B	7.1	6.5	–	11000	61500	–	480	13
C	6.8	5.6	4.6	11000	64000	190000	480	10
D	9.6	4.4	–	9000	72700	–	450	10
E	9.2	3.5	3.4	9000	77500	200000	450	8

vity, respectively, n — electron concentration in QW, μ — mobility of electrons at $B = 0$, e — electron charge, ω_c — cyclotron frequency, τ — transport relaxation time.

Considering that $\omega_c\tau \gg 1$, carrier mobility can be determined based on the slope of the dependencies $\sigma_1^1(1/B^2)$ (see inserts in Figure 5). The results of measurements of the electrophysical parameters of the two-dimensional channel of $In_{0.75}Ga_{0.25}As$ by the van der Pauw method at $T = 80$ and 300 K (for samples A–E), as well as by non-contact acoustic method at $T = 1.7$ K (for samples A, C and E) are provided in Table 2.

A number of the following conclusions can be drawn by comparing the design and conditions of the MBE growth of the structures studied in the paper (see Table 1, the conditions of the MBE growth are duplicated for convenience in Table 2) with their electrophysical characteristics (see Table 2). An increase of the thickness of the lower SL of 1 nm–InAs/4 nm–$In_{0.7}Al_{0.3}As$ (in the case of samples A and B) from 40 to 60 nm results in a slight decrease of the concentration of carriers in the two-dimensional channel of $In_{0.75}Ga_{0.25}As$ from $8.1 \cdot 10^{11}$ to $7.1 \cdot 10^{11}$ cm^{-2} and from $6.7 \cdot 10^{11}$ to $6.5 \cdot 10^{11}$ cm^{-2} at $T = 300$ and 80 K, respectively, due to the reduction of the probability of the overshooting of carriers localized near the MBL/VS, in $In_{0.75}Ga_{0.25}As$ QW. At the same time, the mobility of the carriers at room temperature remains unchanged and is equal to ~ 11000 cm^2/(B · c). The lower electron mobility in the 2D channel in the sample B compared with the sample A at $T = 80$ K is attributable to the development of the surface relief during the growth of the SL caused by suboptimal MBE conditions ($T_s = 480$°C, As_4/III = 13) and, as a result, an increased contribution of scattering on the roughness of the interface of $In_{0.75}Ga_{0.25}As$/(In,Al)As. Earlier, a decrease of electron mobility in $In_{0.7}Ga_{0.3}As/In_{0.64}Al_{0.36}As$ QW due to scattering on the interface roughness was reported in Ref. [16]. The reduction of the ratio of streams of As_4/III from 13 to 10 at constant growth temperature of $T_s = 480$°C of QW and the design of the structure as a whole (sample C) allowed obtaining the concentration of electrons in the 2D channel of $In_{0.75}Ga_{0.25}As$, not exceeding $6.8 \cdot 10^{11}$, $5.6 \cdot 10^{11}$ and $4.6 \cdot 10^{11}$ cm^{-2} at $T = 300$, 80 and 1.7 K, respectively, as well as increased the carrier mobility at $T = 80$ K up to 64 000 cm^2/(B · c).

Several papers [17,18] reported that the scattering over the fluctuations in the composition of solid solutions is main mechanism reducing electron mobility in undoped InGaAs/InAlAs QW. It was assumed that the use of SL of $InAs/In_{0.7}Al_{0.3}As$ as barrier layers for $In_{0.75}Ga_{0.25}As$ QW would reduce the contribution of this scattering mechanism in the structures studied in this paper. Nevertheless, the electron mobility values achieved at $T = 80$ K in the sample D containing a triple solid solution of $In_{0.75}Al_{0.25}As$ as barrier layers were not lower than the values in the samples, containing SL of $InAs/In_{0.7}Al_{0.3}As$. At the same time, the twofold increase of the lower barrier layer thickness (up to 120 nm), as well as a decrease of the growth temperature of the barrier layers and QW to $T_s = 450$°C with a stream ratio of As_4/III equal to 10, allowed obtaining the concentration of carriers in the channel not exceeding $4.4 \cdot 10^{11}$ cm^{-2} at $T = 80$ K. The lowest carrier concentration in the two-dimensional channel ($3.5 \cdot 10^{11}$ and $3.4 \cdot 10^{11}$ cm^{-2} at $T = 80$ and 1.7 K, respectively) was achieved in sample E, the only difference from the sample D consisted in using a lower stream ratio As_4/III = 8 during the QW and barrier layer growth. In addition, this sample demonstrated the highest electron mobility among all studied structures that was equal to 77 500 cm^2/(B · c) at $T = 80$ K. Increased electron concentration at room temperature in the two-dimensional channel of samples D and E compared with samples A, B and C is explained by the absence of SL of $InAs/In_{0.7}Al_{0.3}As$, in which InAs layers localize part of the electrons. In addition, it was shown in [19] that InAs layers can act as barriers to the propagation of optical phonons, thereby reducing electron-phonon scattering in QW, which explains the lower mobility of carriers at room temperature in samples D and E (9000 cm^2/(B · c)) compared to samples A, B and C (11 000 cm^2/(B · c)). It should be noted that all structures studied in this paper at $T = 1.7$ K (samples A, C and E) are characterized by high values of carrier mobility in the 2D channel of $In_{0.75}Ga_{0.25}As$ (190 000–210 000 cm^2/(B · c)), which is at the level of the world's best results. The lower carrier

mobility at $T = 1.7$ K in sample C ($190\,000\,\mathrm{cm}^2/(\mathrm{B}\cdot\mathrm{c})$ at $n = 4.6\cdot10^{11}\,\mathrm{cm}^{-2}$) compared with samples A and E, is most likely explained by the contribution of intersubband carrier scattering, which, as shown in Ref. [17], is maximal with a carrier concentration of $n \sim (3.7{-}4.0)\cdot10^{11}\,\mathrm{cm}^{-2}$

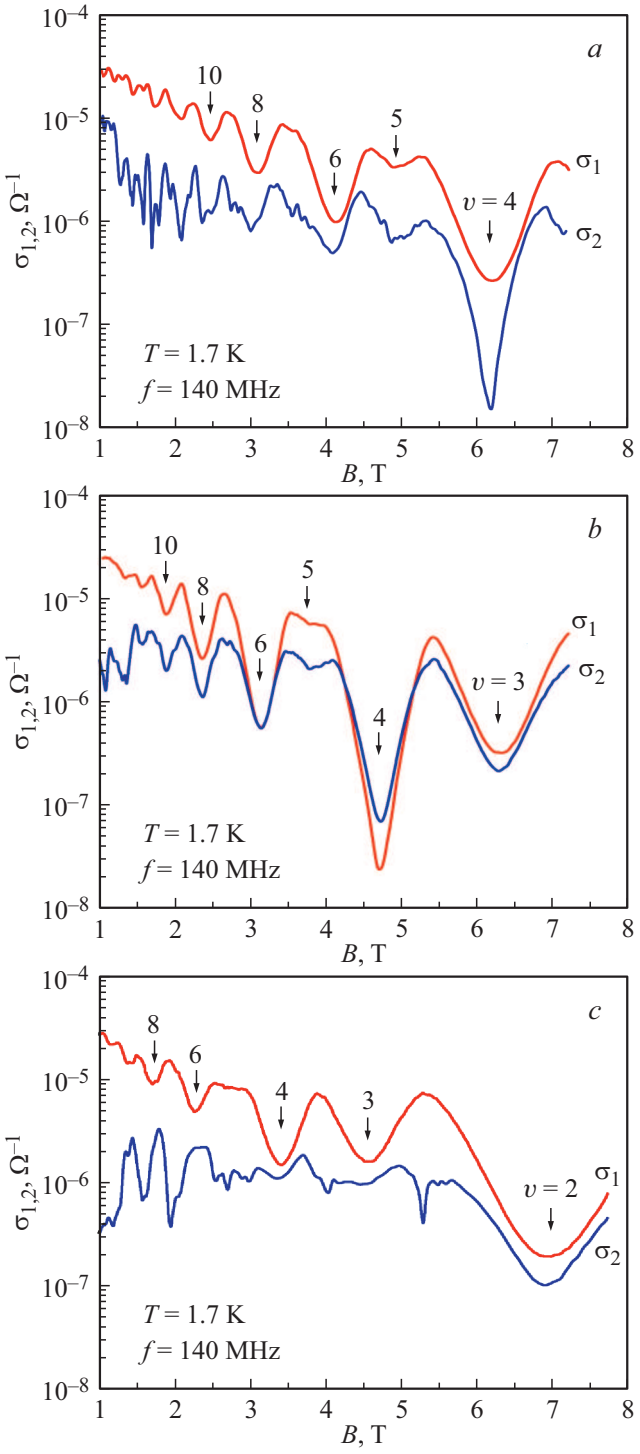

Figure 4. Dependences of the real (σ_1) and imaginary (σ_2) parts of the high-frequency conductivity on the magnetic field for samples A (a), C (b) and E (c) at $T = 1.7$ K and SAW frequency of $f = 140$ MHz. The arrows show the occupation numbers (ν).

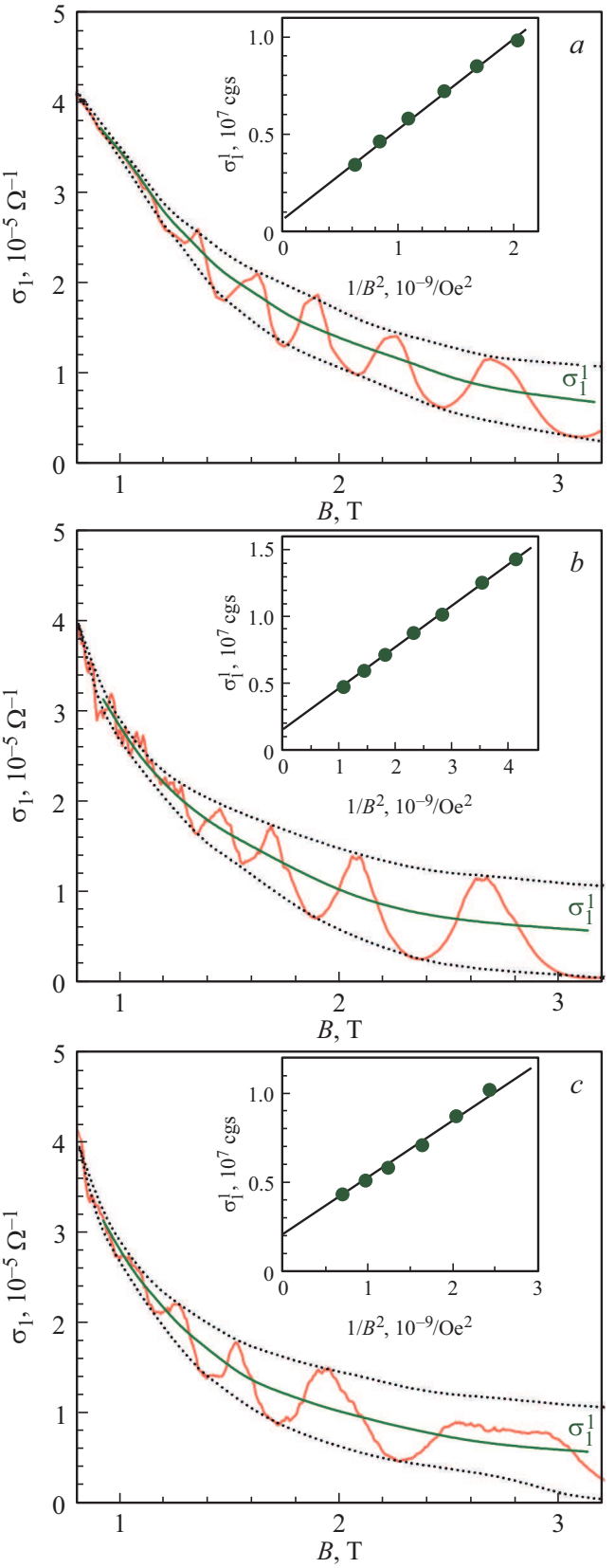

Figure 5. Dependences of the non-oscillating part of the conductivity (σ_1^1) on the magnetic field for samples A (a), C (b) and E (c) at T=1.7 K and SAW frequency of f=140 MHz. Dependencies $\sigma_1^1(1/B^2)$, the slope of which determined the mobility of the carriers are shown on the inserts.

and corresponds to the occupation of the second energy level in the QW.

4. Conclusion

30 nm thick metamorphic heterostructures with $In_{0.75}Ga_{0.25}As$ QW and different barrier layer designs (In,Al)As were obtained by the MBE method on GaAs(001) substrates. It was found that the use of SL of $InAs/In_{0.7}Al_{0.3}As$ as barrier layers reduces the concentration of electrons in the two-dimensional channel of $In_{0.75}Ga_{0.25}As$ and increases their mobility at room temperature because part of the carriers and optical phonons are captured by InAs layers. In addition, it was shown that an increase of the thickness of the lower barrier layer from 40 to 120 nm in combination with the use of optimal modes of MBE growth ($T_s = 450^\circ C$; $As_4/III = 8$) of $In_{0.75}Ga_{0.25}As/In_{0.75}Al_{0.25}As$ QW allows obtaining electron concentration values in the 2D channel of $\leq 3.5 \cdot 10^{11}\,cm^{-2}$ at $T \leq 80\,K$, which corresponds to occupation of only the first level of dimensional quantization, as well as the mobility of electrons of $\geq 77\,500$ and $200\,000\,cm^2/(B \cdot c)$ at $T = 80$ and 1.7 K, respectively, due to the suppression of contributions of intersubband scattering and carrier scattering on the roughness of QW interfaces. The results obtained indicate the prospects of such heterostructures both for studying fundamental spin phenomena and for creating QW structures of HEMT transistors based on them using modulated doping.

Funding

M.Yu. Chernov thanks the Russian Science Foundation (grant No. 22-79-00265) for partial support of these studies.

Conflict of interest

The authors declare that they have no conflict of interest.

References

[1] J.Y. Park, B.-G. Min, J.-M. Lee, W. Chang, D.M. Kang, E-S. Jang, J. Kim, J.-G. Kim. Electron. Lett., **59** (14), e12886 (2023).
[2] J. Ajayan, T. Ravichandran, P. Mohankumar, P. Prajoon, J.C. Pravin, D. Nirmal. IETE J. Res., **67** (3), 366 (2021).
[3] J. A. del Alamo. Nature, **479**, 317 (2011).
[4] F. Heinz, F. Thorne, A. Leuther, O. Ambacher. IEEE Trans. Microwave Theory Techniques, **69** (8), 3896 (2021).
[5] S.V. Ivanov, M.Yu. Chernov, V.A. Solov'ev, P.N. Brunkov, D.D. Firsov, O.S. Komkov. Progr. Cryst. Growth Charact. Mater., **65** (1), 20 (2019).
[6] F. Capotondi, G. Biasiol, I. Vobornik, L. Sorba, F. Giazotto, A. Cavallini, B. Fraboni. J. Vac. Sci. Technol. B, **22**, 702 (2004).
[7] M.Yu. Chernov, O.S. Komkov, D.D. Firsov, B.Ya. Meltser, A.N. Semenov, Ya.V. Terent'ev, P.N. Brunkov, A.A. Sitnikova, P.S. Kop'ev, S.V. Ivanov, V.A. Solov'ev. J. Cryst. Growth, **477** (1), 97 (2017).
[8] V.A. Solov'ev, M.Yu. Chernov, M.V. Baidakova, D.A. Kirilenko, M.A. Yagovkina, A.A. Sitnikova, T.A. Komissarova, P.S. Kop'ev, S.V. Ivanov. Superlat. Microstruct., **113**, 777 (2018).
[9] Y. Asaoka. J. Cryst. Growth, **251**, 40 (2003).
[10] V.A. Solov'ev, M.Yu. Chernov, A.A. Sitnikova, P.N. Brunkov, B.Ya. Meltser, S.V. Ivanov. Semiconductors, **52**, 120 (2018).
[11] Yu.G. Galitsin, D.V. Dmitriev, V.G. Mansurov, S.P. Moshchenko, A.I. Toropov. Pisma ZhETF, **84** (9), 596 (2006). (in Russian).
[12] I.L. Drichko, I.Yu. Smirnov. Semiconductors, **31**, 933 (1997).
[13] V.D. Kagan. Semiconductors, **31**, 407 (1997).
[14] I.L. Drichko, A.M. Diakonov, I.Y. Smirnov, Y.M. Galperin, A.I. Toropov. Phys. Rev. B, **62**, 7470 (2000).
[15] T. Ando. J. Phys. Soc. Jpn., **37**, 1233 (1974).
[16] G.B. Galiev, I.S. Vasil'evskii, E.A. Klimov, S.S. Pushkarev, A.N. Klochkov, P.P. Maltsev, M.Yu. Presniakov, I.N. Trunkin, A.L. Vasiliev. J. Cryst. Growth, **392**, 11 (2014).
[17] F. Capotondi. G. Biasiol, D. Ercolani, L. Sorba. J. Cryst. Growth, **278**, 538 (2005).
[18] S. Gozu, K. Tsuboki, M. Hayashi, C. Hong, S. Yamada. J. Cryst. Growt, **201**–**202**, 749 (1999).
[19] A. Shilenas, Yu. Pozhela, K. Pozhela, V. Yutsen, I.S. Vasilevsky, G.B. Galiev, S.S. Pushkarev, E.A. Klimov. FTP, **47** (3), 348 (2013). (in Russian).

Translated by A.Akhtyamov